Magnetohydrodynamic Flow of a Carreau Fluid in a Channel with Different Wave Forms

Tasawar Hayat[a,b], Najma Saleem[a], Said Mesloub[b], and Nasir Ali[c]

[a] Department of Mathematics, Quaid-i-Azam University, Islamabad 44000, Pakistan
[b] Department of Mathematics, King Saud University Riyadh 11451, Saudi Arabia
[c] Faculty of Basic and Applied Sciences, International Islamic University, Islamabad 44000, Pakistan

Reprint requests to T. H.; E-mail: pensy_t@yahoo.com

Z. Naturforsch. **66a,** 215 – 222 (2011); received March 16, 2009 / revised February 16, 2011

In this investigation, we discuss the peristaltic motion based on the constitutive equations of a Carreau fluid in a channel. The fluid is electrically conducting in the presence of a uniform applied magnetic field. Four different wave forms are chosen. The fluid behaviour is studied using long wavelength approximation. Detailed analysis is performed for various emerging parameters on pumping and trapping phenomena. The present results reduce favourably with the currently available results of hydrodynamic case when the Hartman number is chosen zero.

Key words: Symmetric Channel; Magnetic Field; Trapping.

1. Introduction

Over the past four decades, the peristaltic motion have been looked in the biological sciences in general and the physiology in particular. Particularly in physiological flows, the peristaltic motion occurs in urine transport, swallowing of foods through the oesophagus, movement of chyme in the intestine, the movement of ovum in the female fallopian tube, the vasomotion in small blood vessels, and many others. Furthermore, roller and finger pumps also work according to the principle of peristaltic transport. A vast amount of existing literature on peristaltic motion involves the viscous fluid under several geometries and assumptions. Not much has been reported relevant to the peristaltic motion of non-Newtonian fluids in hydrodynamic situations. In fact this is due to the reason that the non-Newtonian fluids have fairly complicated constitutive equations which add more terms and increase the order of the governing equations. In view of all these complexities, some recent investigations describing the process of peristalsis under one or more simplified assumptions have been presented in the studies [1 – 30]. From the existing literature it is noticed that investigations on the peristalsis in regime of magnetohydrodynamics (MHD) are scant in comparison to the hydrodynamics.

The main theme of the present study is to putforward the MHD flow analysis of peristaltic transport non-Newtonian fluids. In the present study, constitutive equations in a Carreau fluid are employed. Mathematical analysis has been carried out by using long wavelength and low Reynolds number approximations. The magnetic Reynolds number is selected small and the induced magnetic field is neglected. Important flow features of Hartman number on the velocity, pressure gradient, trapping, and pumping phenomena are discussed.

2. Theory

We analyze the flow of an incompressible Carreau fluid in a two dimensional channel of width $2a$. The flow is induced by a periodic peristaltic wave of wavelength λ. A wave of amplitude b propagates along the channel walls with constant speed c. Its instantaneous height at any axial station X' is

$$EY' = H\left(\frac{X' - ct'}{\lambda}\right). \tag{1}$$

Four possible wave forms, namely sinusoidal (s), triangular (t), square (sq), and trapezoidal (tr), are considered. A constant magnetic field $\mathbf{B}_0$ is applied in the y-direction. An induced magnetic field is taken

negligible under the assumption of small magnetic Reynolds number. Furthermore the electric field is chosen zero. It is further noticed that flow in laboratory (X',Y') and wave (x',y') frames are treated unsteady and steady, respectively. The transformations between the two frames are in the form

$$\begin{aligned} x' &= X' - ct', \qquad y' = Y', \\ u'(x',y') &= U' - c, \qquad v'(x',y') = V', \end{aligned} \tag{2}$$

in which (U',V') and (u',v') are the respective velocities in the laboratory and wave frames.

In the absence of infinite shear stress viscosity, the extra stress tensor $\overline{\tau}$ is

$$\overline{\tau} = -\left[\eta_0\left(1+\left(\Gamma\,\overline{\dot{\gamma}}\right)^2\right)^{\frac{n-1}{2}}\right]\overline{\dot{\gamma}}, \tag{3}$$

$$\overline{\dot{\gamma}} = \sqrt{\frac{1}{2}\sum_i\sum_j \overline{\dot{\gamma}}_{ij}\overline{\dot{\gamma}}_{ji}} = \sqrt{\frac{1}{2}\pi}, \tag{4}$$

where η_0 is the zero shear-rate viscosity, Γ the time constant, n the dimensionless power law index, and π the second invariant of strain-rate tensor. It should be pointed out that for $n=1$ or $\Gamma=0$ (3) corresponds to the Newtonian fluid.

The relevant equations are

$$\nabla\cdot\overline{\mathbf{V}}' = 0, \tag{5}$$

$$\rho\left[\frac{\partial}{\partial t} + (\overline{\mathbf{V}}'\cdot\nabla)\right]\overline{\mathbf{V}}' = -\overline{\nabla}p' + \operatorname{div}\,\overline{\tau}' + \mathbf{J}\times\mathbf{B}. \tag{6}$$

In the above expressions p' is the fluid pressure, $\mathbf{J}$ the current density, $\mathbf{B}$ the total magnetic field, and the velocity $\overline{\mathbf{V}}'$ is given by

$$\overline{\mathbf{V}}' = (u',v',0). \tag{7}$$

In view of following dimensionless variables, we set

$$\begin{aligned} &x = \frac{x'}{\lambda},\ y = \frac{y'}{a},\ u = \frac{u'}{c},\ v = \frac{v'}{\delta c},\ t = \frac{t'c}{\lambda}, \\ &h = \frac{H}{a},\ \delta = \frac{a}{\lambda},\ \mathrm{Re} = \frac{\rho ca}{\eta_0},\ p = \frac{a^2p'}{c\lambda\eta_0}, \\ &\mathrm{We} = \frac{\Gamma c}{a},\ \Phi = \frac{a}{b},\ \tau_{xx} = \frac{\lambda\tau'_{xx}}{\eta_0 c},\ \tau_{xy} = \frac{a\tau'_{xy}}{\eta_0 c}, \\ &\tau_{yy} = \frac{a\tau'_{yy}}{\eta_0 c},\ M^2 = \frac{\sigma B_0'^2 a^2}{\eta_0}, \end{aligned} \tag{8}$$

and define the stream function $\Psi(x,y)$ by

$$u = \frac{\partial\Psi}{\partial y},\ v = -\delta\frac{\partial\Psi}{\partial x}. \tag{9}$$

We find that (5) is identically satisfied and (6) becomes

$$\begin{aligned} &\delta\mathrm{Re}\left[\left(\frac{\partial\Psi}{\partial y}\frac{\partial}{\partial x} - \frac{\partial\Psi}{\partial x}\frac{\partial}{\partial y}\right)\frac{\partial\Psi}{\partial y}\right] \\ &= -\frac{\partial p}{\partial x} - \frac{\delta^2}{2}\frac{\partial\tau_{xx}}{\partial x} - \frac{\partial\tau_{xy}}{\partial y} - M^2\frac{\partial\Psi}{\partial y}, \end{aligned} \tag{10}$$

$$\begin{aligned} &-\delta^3\mathrm{Re}\left[\left(\frac{\partial\Psi}{\partial y}\frac{\partial}{\partial x} - \frac{\partial\Psi}{\partial x}\frac{\partial}{\partial y}\right)\frac{\partial\Psi}{\partial x}\right] \\ &= -\frac{\partial p}{\partial y} - \delta^2\frac{\partial\tau_{xy}}{\partial x} - \delta\frac{\partial\tau_{yy}}{\partial y} + \delta M^2\frac{\partial\Psi}{\partial x}, \end{aligned} \tag{11}$$

where

$$\tau_{xx} = -2\left[1+\frac{(n-1)}{2}\mathrm{We}^2\dot{\gamma}^2\right]\frac{\partial^2\Psi}{\partial x\partial y}, \tag{12}$$

$$\tau_{xy} = -\left[1+\frac{(n-1)}{2}\mathrm{We}^2\dot{\gamma}^2\right]\left(\frac{\partial^2\Psi}{\partial y^2} - \delta^2\frac{\partial^2\Psi}{\partial x^2}\right), \tag{13}$$

$$\tau_{yy} = 2\delta\left[1+\frac{(n-1)}{2}\mathrm{We}^2\dot{\gamma}^2\right]\frac{\partial^2\Psi}{\partial x\partial y}, \tag{14}$$

$$\begin{aligned} \dot{\gamma} = \Bigg[&2\delta^2\left(\frac{\partial^2\Psi}{\partial x\partial y}\right)^2 + \left(\frac{\partial^2\Psi}{\partial y^2} - \delta^2\frac{\partial^2\Psi}{\partial x^2}\right)^2 \\ &+ 2\delta^2\left(\frac{\partial^2\Psi}{\partial x\partial y}\right)^2\Bigg]^{\frac{1}{2}}, \end{aligned} \tag{15}$$

in which We is the Wessinberg number, Re the Reynolds number, and M the Hartman number.

Under the assumptions of long wavelength [31 – 40] and low Reynolds number, (10) and (11) after using (13) become

$$\begin{aligned} \frac{\partial p}{\partial x} = &\frac{\partial}{\partial y}\left[1+\frac{(n-1)}{2}\mathrm{We}^2\left(\frac{\partial^2\Psi}{\partial y^2}\right)^2\right]\frac{\partial^2\Psi}{\partial y^2} \\ &- M^2\frac{\partial\Psi}{\partial y}, \end{aligned} \tag{16}$$

$$\frac{\partial p}{\partial y} = 0. \tag{17}$$

Eliminating pressure p from (16), we get

$$\begin{aligned} &\frac{\partial^2}{\partial y^2}\left[1+\frac{(n-1)}{2}\mathrm{We}^2\left(\frac{\partial^2\Psi}{\partial y^2}\right)^2\right]\frac{\partial^2\Psi}{\partial y^2} \\ &- M^2\frac{\partial^2\Psi}{\partial y^2} = 0, \end{aligned} \tag{18}$$

and (17) shows that $p \neq p(y)$.

In a wave frame, the dimensionless boundary conditions and pressure rise per wavelength Δp_λ are

$$\Psi = 0,\ \frac{\partial^2 \Psi}{\partial y^2} = 0 \ \text{ at } y = 0, \tag{19}$$

$$\Psi = F,\ \frac{\partial \Psi}{\partial y} = -1 \ \text{ at } y = h, \tag{20}$$

$$\Delta p_\lambda = \int_0^1 \left(\frac{\mathrm{d}p}{\mathrm{d}x}\right)\mathrm{d}x. \tag{21}$$

The dimensionless mean flows in laboratory (θ) and wave (F) frames are related by the following expressions:

$$\theta = F + 1, \tag{22}$$

$$F = \int_0^h \frac{\partial \Psi}{\partial y}\mathrm{d}y. \tag{23}$$

3. Perturbation Solution

For small We we may write

$$\Psi = \Psi_0 + \mathrm{We}^2\Psi_1 + O(\mathrm{We}^4), \tag{24}$$

$$F = F_0 + \mathrm{We}^2 F_1 + O(\mathrm{We}^4), \tag{25}$$

$$p = p_0 + \mathrm{We}^2 p_1 + O(\mathrm{We}^4). \tag{26}$$

Substituting (24)–(26) into (16), (18) and (19)–(23), solving the resulting systems and then neglecting the terms of order greater than We^2, we get

$$\Psi = \Psi_0 + \mathrm{We}^2\Psi_1, \tag{27}$$

$$\frac{\mathrm{d}p}{\mathrm{d}x} = \frac{\mathrm{d}p_0}{\mathrm{d}x} + \mathrm{We}^2\frac{\mathrm{d}p_1}{\mathrm{d}x}, \tag{28}$$

$$\Delta p_\lambda = \Delta p_{\lambda_0} + \mathrm{We}^2\Delta p_{\lambda_1}, \tag{29}$$

where

$$\begin{aligned}\Psi_0 = {} & \left(\frac{F_0 M + \tanh Mh}{Mh - \tanh Mh}\right)\left\{y - \frac{\sinh My}{M\cosh Mh}\right\} \\ & - \frac{\sinh My}{M\cosh Mh},\end{aligned} \tag{30}$$

$$\begin{aligned}\Psi_1 = {} & \frac{F_1 yM\cosh Mh}{Mh\cosh Mh - \sinh Mh} \\ & - \frac{(n-1)\left(\frac{\mathrm{d}p_0}{\mathrm{d}x} - M^2\right)^3 My\cosh Mh}{\cosh Mh^3(Mh\cosh Mh - \sinh Mh)} \\ & \cdot\left\{\frac{3h\cosh 3Mh}{64M^4} - \frac{\sinh 3Mh}{64M^5} - \frac{3h^2\sinh Mh}{16M^3}\right\} \\ & - \frac{(n-1)\left(\frac{\mathrm{d}p_0}{\mathrm{d}x} - M^2\right)^3 y}{\cosh Mh^3 Mh} \\ & \cdot\left\{\frac{-3\cosh 3Mh}{64M^4} + \frac{3\cosh Mh}{16M^4} + \frac{3h\sinh Mh}{16M^3}\right\} \\ & - \frac{F_1\sinh My}{Mh\cosh Mh - \sinh Mh} \\ & + \frac{(n-1)\left(\frac{\mathrm{d}p_0}{\mathrm{d}x} - M^2\right)^3\sinh My}{\cosh Mh^3(Mh\cosh Mh - \sinh Mh)} \\ & \cdot\left\{\frac{3h\cosh 3Mh}{64M^4} - \frac{\sinh 3Mh}{64M^5} - \frac{3h^2\sinh Mh}{16M^3}\right\} \\ & + \frac{(n-1)\left(\frac{\mathrm{d}p_0}{\mathrm{d}x} - M^2\right)^3}{\cosh Mh^3 Mh}\left\{-\frac{\sinh 3My}{64M^5} + \frac{3y\cosh My}{16M^4}\right\},\end{aligned} \tag{31}$$

$$\frac{\mathrm{d}p_0}{\mathrm{d}x} = -M^2\left(\frac{MF_0 + \tanh Mh}{Mh - \tanh Mh}\right), \tag{32}$$

$$\begin{aligned}\frac{\mathrm{d}p_1}{\mathrm{d}x} = {} & -\frac{F_1 M^3\cosh Mh}{Mh\cosh Mh - \sinh Mh} \\ & + \frac{(n-1)\left(\frac{\mathrm{d}p_0}{\mathrm{d}x} - M^2\right)^3}{\cosh Mh^2(Mh\cosh Mh - \sinh Mh)} \\ & \cdot\left\{\frac{3h\cosh 3Mh}{64M} - \frac{\sinh 3Mh}{64M^2} - \frac{3h^2\sinh Mh}{16}\right\} \\ & + \frac{(n-1)\left(\frac{\mathrm{d}p_0}{\mathrm{d}x} - M^2\right)^3}{\cosh Mh^3 Mh} \\ & \cdot\left\{\frac{3\cosh Mh}{16M^2} - \frac{3\cosh 3Mh}{64M^2} + \frac{3h\sinh Mh}{16M}\right\},\end{aligned} \tag{33}$$

$$\Delta p_{\lambda_0} = \int_0^1 \frac{\mathrm{d}p_0}{\mathrm{d}x}\mathrm{d}x, \tag{34}$$

$$\Delta p_{\lambda_1} = \int_0^1 \frac{\mathrm{d}p_1}{\mathrm{d}x}\mathrm{d}x. \tag{35}$$

The stream function Ψ is

$$\begin{aligned}\Psi = {} & \left(\frac{FM + \tanh Mh}{Mh - \tanh Mh}\right)\left\{y - \frac{\sinh My}{M\cosh Mh}\right\} \\ & - \frac{\sinh My}{M\cosh Mh} \\ & - \frac{\mathrm{We}^2(n-1)\left(\left(\frac{M^3F + M^2\tanh Mh}{Mh - \tanh Mh}\right) - M^2\right)^3 My\cosh Mh}{\cosh Mh^3(Mh\cosh Mh - \sinh Mh)} \\ & \cdot\left\{\frac{3h\cosh 3Mh}{64M^4} - \frac{\sinh 3Mh}{64M^5} - \frac{3h^2\sinh Mh}{16M^3}\right\} \\ & - \frac{\mathrm{We}^2(n-1)\left(\left(\frac{M^3F + M^2\tanh Mh}{Mh - \tanh Mh}\right) - M^2\right)^3 y}{\cosh Mh^3 Mh}\end{aligned}$$

$$\cdot\left\{\frac{-3\cosh 3Mh}{64M^4}+\frac{3\cosh Mh}{16M^4}+\frac{3h\sinh Mh}{16M^3}\right\}$$
$$+\frac{\mathrm{We}^2(n-1)\left(\left(\frac{M^3F+M^2\tanh Mh}{Mh-\tanh Mh}\right)-M^2\right)^3\sinh My}{\cosh Mh^3(Mh\cosh Mh-\sinh Mh)}$$
$$\cdot\left\{\frac{3h\cosh 3Mh}{64M^4}-\frac{\sinh 3Mh}{64M^5}-\frac{3h^2\sinh Mh}{16M^3}\right\}$$
$$+\frac{\mathrm{We}^2(n-1)\left(\left(\frac{M^3F+M^2\tanh Mh}{Mh-\tanh Mh}\right)-M^2\right)^3}{\cosh Mh^3 Mh}$$
$$\cdot\left\{\frac{3y\cosh My}{16M^4}-\frac{\sinh 3My}{64M^5}\right\}. \tag{36}$$

4. Expressions for Wave Shape

The nondimensional expressions of the considered wave forms are given by the following equations:

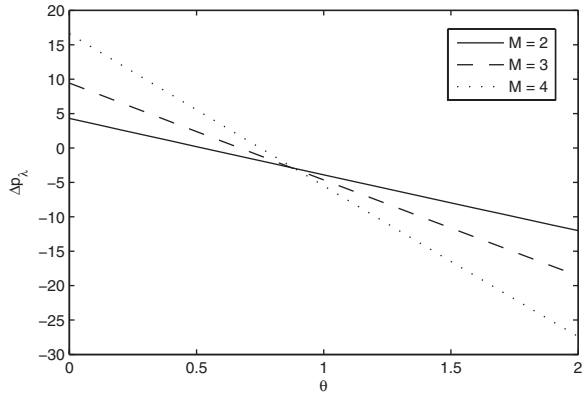

Fig. 1. Plot showing Δp_λ versus flow rate θ for sinusoidal wave. Here $\Phi = 0.2$, We $= 0.4$, and $n = 0.398$.

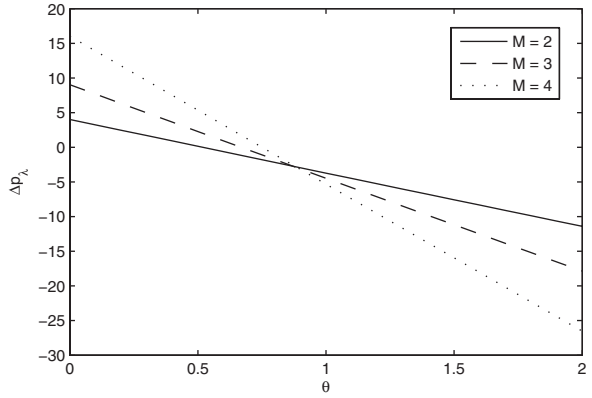

Fig. 2. Plot showing Δp_λ versus flow rate θ for triangular wave. Here $\Phi = 0.2$, We $= 0.4$, and $n = 0.398$.

(1) Sinusoidal wave

$$h(x) = 1 + \Phi \sin 2\pi x.$$

(2) Triangular wave

$$h(x) = 1 + \Phi\left[\frac{8}{\pi^3}\sum_{m=1}^{\infty}\frac{(-1)^{m+1}}{(2m-1)^2}\sin\{2(2m-1)\pi x\}\right].$$

(3) Square wave

$$h(x) = 1 + \Phi\left[\frac{4}{\pi}\sum_{m=1}^{\infty}\frac{(-1)^{m+1}}{(2m-1)}\cos\{2(2m-1)\pi x\}\right].$$

(4) Trapezoidal wave

$$h(x) = 1 + \Phi\left[\frac{32}{\pi^2}\sum_{m=1}^{\infty}\frac{(-1)^{m+1}\sin\{\frac{\pi}{3}(2m-1)\}}{(2m-1)^2}\right.$$
$$\left.\cdot\sin\{2(2m-1)\pi x\}\right].$$

The total number of terms in the series that are incorporated in the analysis are 50. Note that the expressions for triangular, square, and tapezoidal waves are derived from Fourier series.

5. Results and Discussion

Our primary interest in this study is to discuss the salient features of Hartman number M on various flow quantities such as pressure rise Δp_λ per wavelength, longitudinal velocity u, and stream function Ψ. Graphical results presented in Figures 1–10 illustrate these effects.

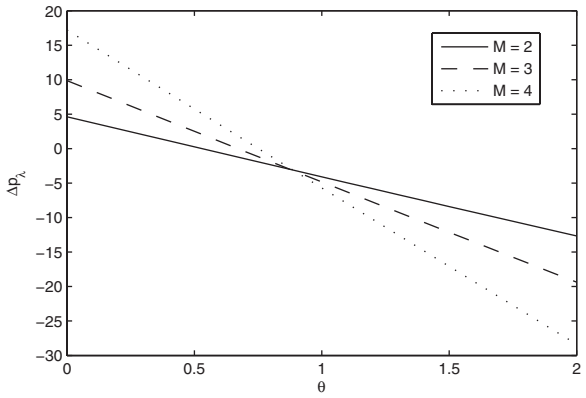

Fig. 3. Plot showing Δp_λ versus flow rate θ for square wave. Here $\Phi = 0.2$, We $= 0.4$, and $n = 0.398$.

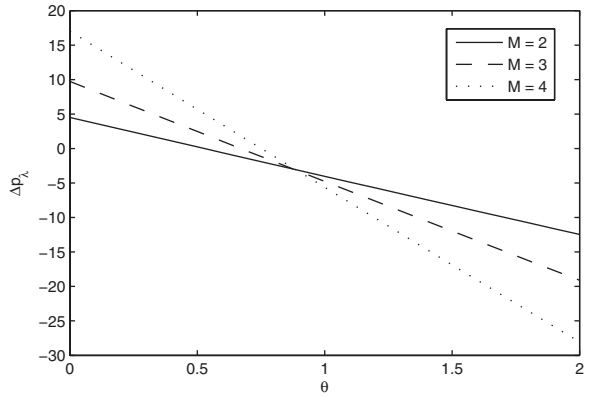

Fig. 4. Plot showing Δp_λ versus flow rate θ for trapezoidal wave. Here $\Phi = 0.2$, We $= 0.4$, and $n = 0.398$.

In Figures 1 – 4 the variation of Δp_λ with the flow rate θ is dislayed for differenet values of M. These figures show that in all the considered wave forms, the Hartman number causes an increase in Δp_λ in pumping as well as in copumping regions. The peristaltic pumping rate and free pumping rate increases with an increase in M. However, in copumping for an appropriate negative value of Δp_λ the flow rate decreases by increasing M. A close look at Figure 2 (which is for triangular wave) reveals that Δp_λ for triangular wave is less in magnitude when compared with other wave forms.

Figure 5 is sketched just to see the influence of M on the longitudinal velocity in the narrow part of the channel for all the considered wave forms. From these figures it is concluded that the longitudinal velocity near the center of the channel decreases by increasing M. However, the opposite behaviour is seen near the wall. A comparison of these figures further reveals that at the channel center, the longitudinal velocity is maximum in the case of sinusoidal and trapezoidal waves.

Figure 6 illustrates the variation of u in the wider part of the channel for all the considered wave forms.

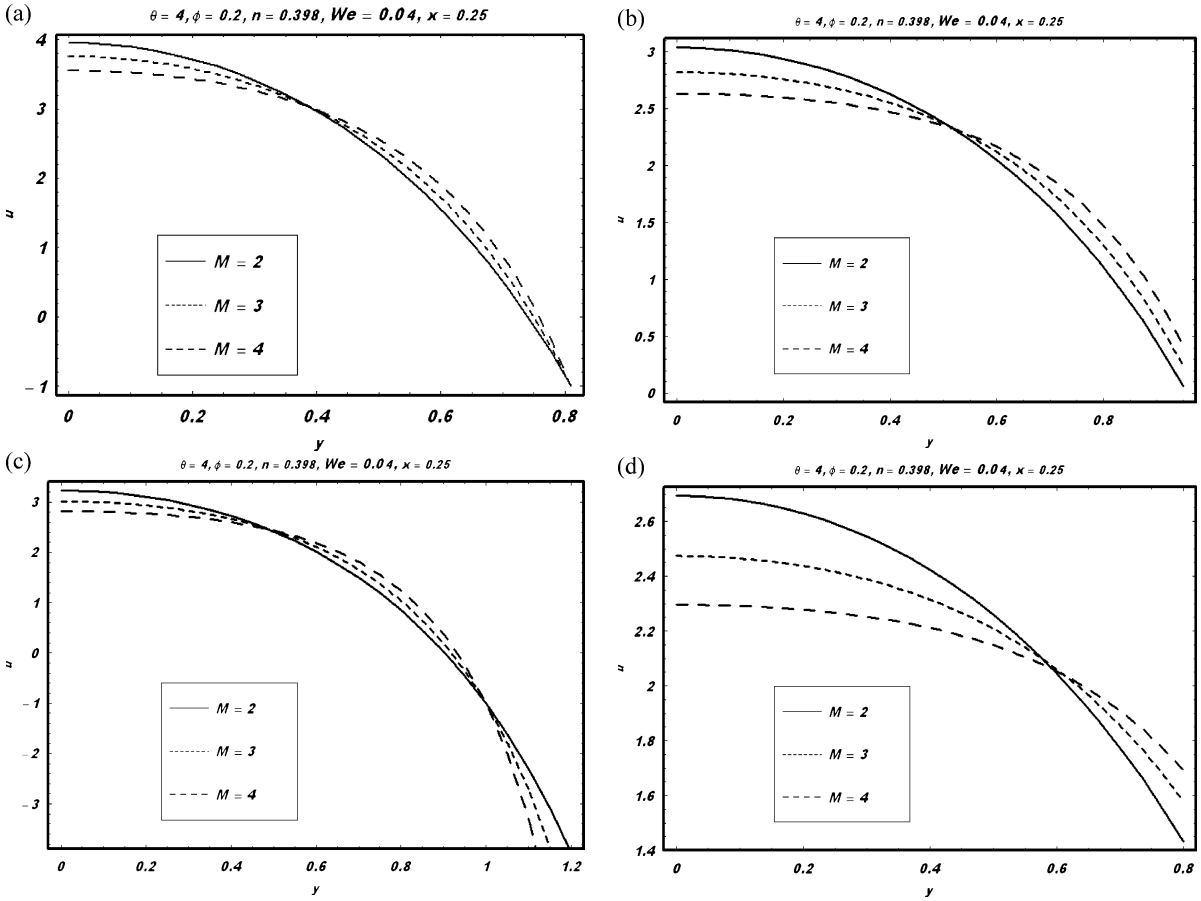

Fig. 5. Plot showing velocity u versus y for narrow part of the channel for (a) sinusoidal wave, (b) triangular wave, (c) square wave, (d) trapezoidal wave.

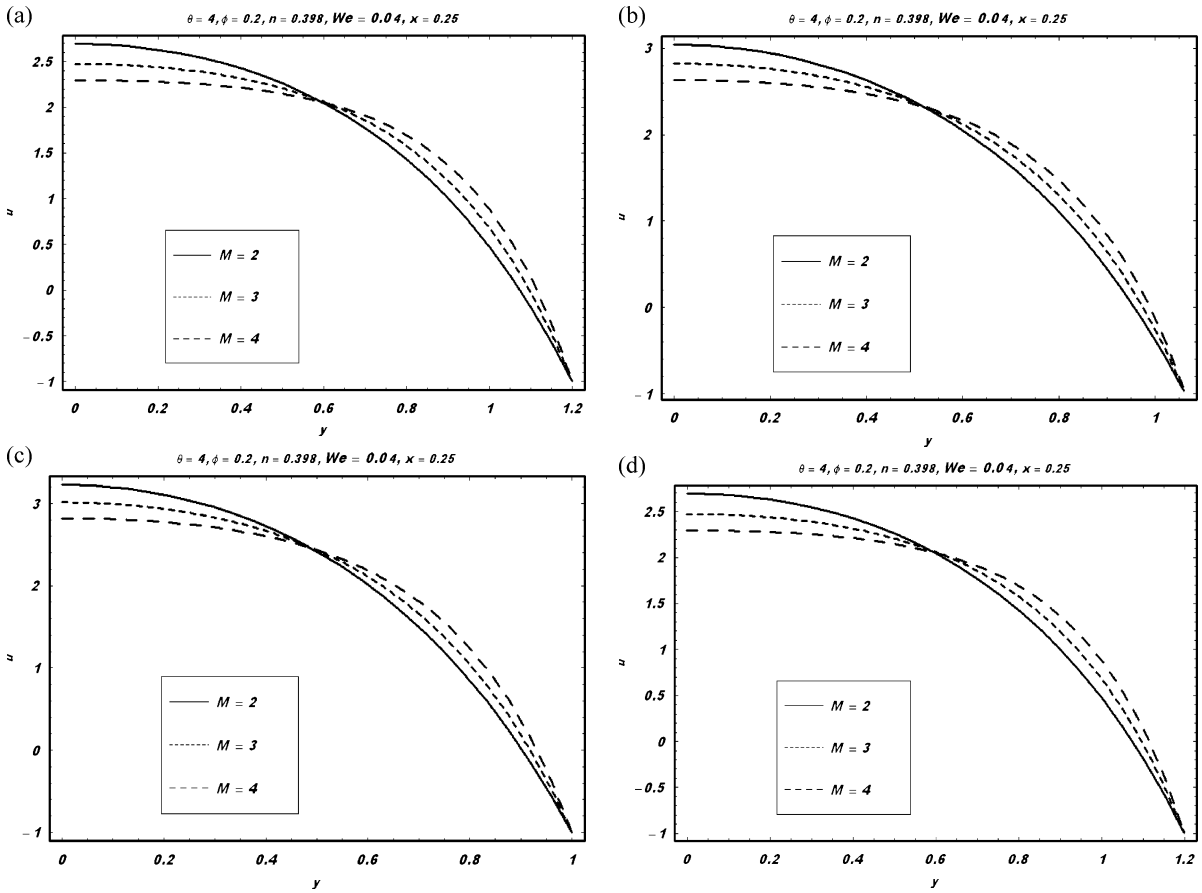

Fig. 6. Plot showing velocity u versus y for wider part of the channel for (a) sinusoidal wave, (b) triangular wave, (c) square wave, (d) trapezoidal wave.

We observe from these figures that the behaviour of velocity in the wider part of the channel is quite similar to that in the narrow part.

To discuss the effects of M on the phenomenon of trapping, we have prepared Figures 7 – 10. These figures reveal that by increasing M the size of the

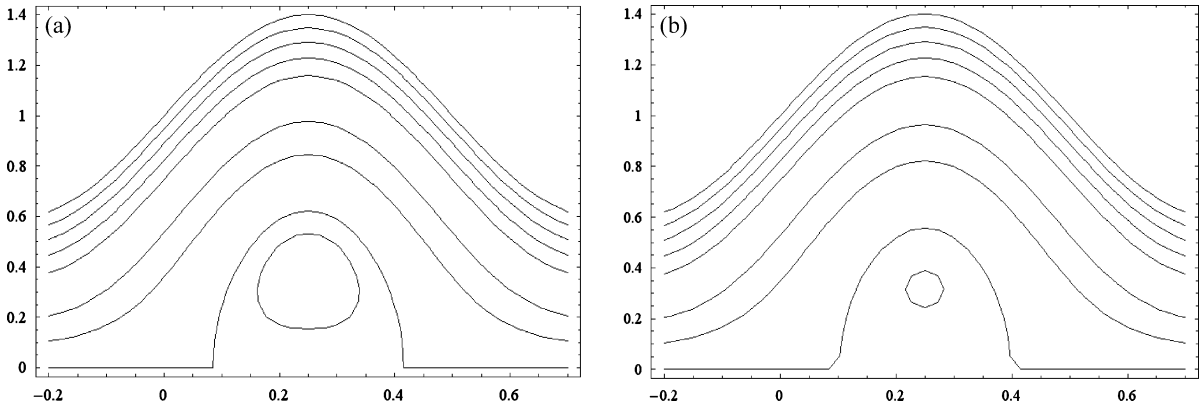

Fig. 7. Streamlines for (a) $M = 0.2$ and (b) $M = 0.8$. The other parameters are $\Phi = 0.4$, $n = 0.398$, We $= 0.04$, $\theta = 0.6$.

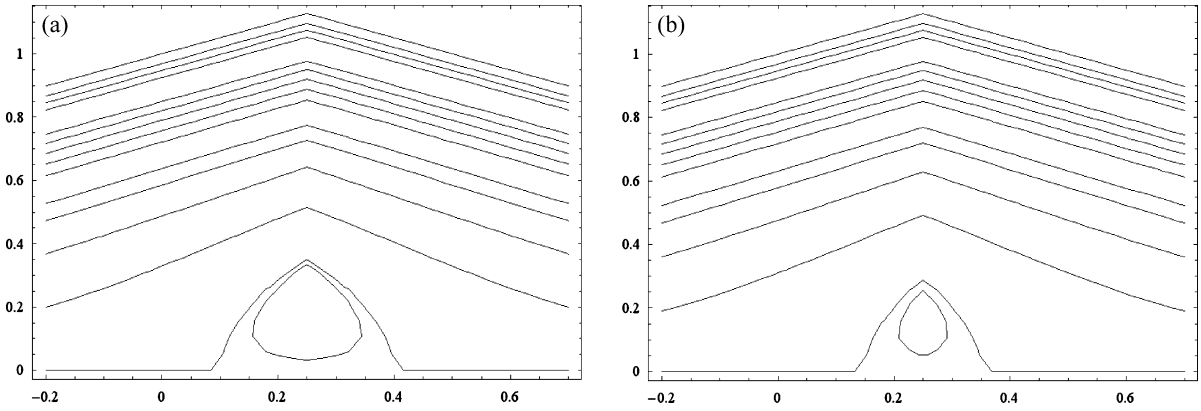

Fig. 8. Streamlines for (a) $M = 0.2$ and (b) $M = 0.8$. The other parameters are $\Phi = 0.4$, $n = 0.398$, We $= 0.04$, $\theta = 0.6$.

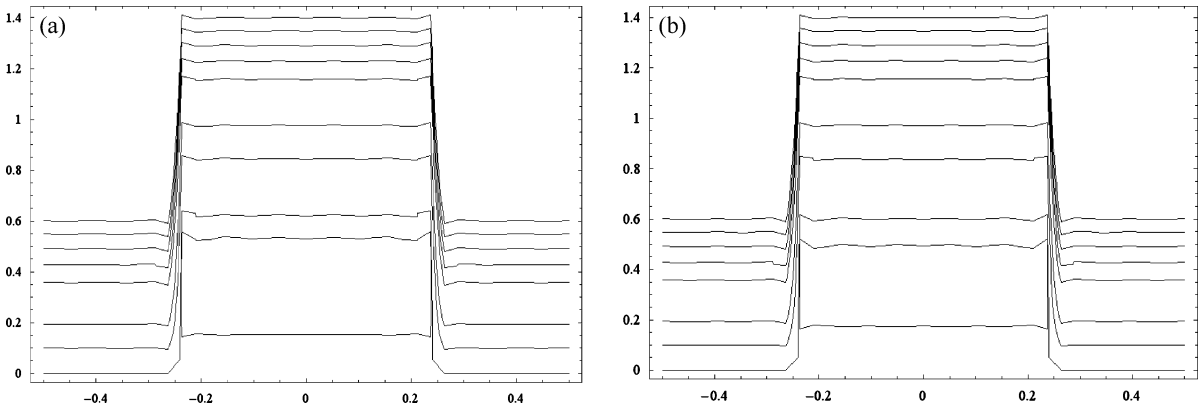

Fig. 9. Streamlines for (a) $M = 0.2$ and (b) $M = 0.8$. The other parameters are $\Phi = 0.4$, $n = 0.398$, We $= 0.04$, $\theta = 0.6$.

trapped bolus decreases and it vanishes when large values of M are taken into account. We have noticed from these figures that the lower trapping limit for triangular wave is less when compared with the other wave forms.

6. Concluding Remarks

An analysis of peristaltic flow of MHD Carreau fluid is presented in a two dimensional channel under long wavelength and low Reynolds number approximations.

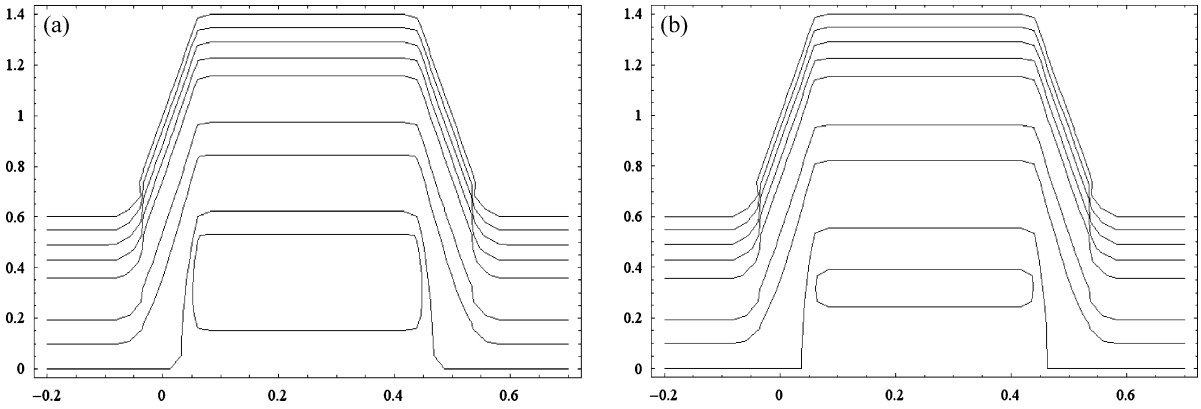

Fig. 10. Streamlines for (a) $M = 0.2$ and (b) $M = 0.8$. The other parameters are $\Phi = 0.4$, $n = 0.398$, We $= 0.04$, $\theta = 0.6$.

Four different wave forms are examined. The effects of Hartman number M on pressure rise per wavelength, longitudinal velocity, and trapping phenomenon are seen through graphs. It is observed that Δp_λ increases by increasing M, and for triangular wave its magnitude is less when compared with the others waves forms. The size of the trapped bolus is a decreasing function of M. The lower trapping limit for triangular wave is less in comparison to the other wave forms.

Acknowledgements

First author gratefully acknowledges the URF from QAU. Prof. Hayat as a visiting professor also thanks the King Saud University for the support (KSU VPP 103).

[1] Kh. S. Mekheimer and Y. A. Elmaboud, Phys. Lett. A **372**, 1657 (2008).
[2] Kh. S. Mekheimer, Phys. Lett. A **372**, 4271 (2008).
[3] Kh. S. Mekheimer and Y. A. Elmaboud, Physica A **387**, 2403 (2008).
[4] M. H. Haroun, Comm. Nonlinear Sci. Numer. Simul. **12**, 1464 (2007).
[5] M. H. Haroun, Comput. Mat. Sci. **39**, 324 (2007).
[6] M. Elshahed and M. H. Haroun, Math. Prob. Eng. **6**, 663 (2005).
[7] T. Hayat and N. Ali, Physica A **370**, 225 (2006).
[8] T. Hayat and N. Ali, Math. Computer Modeling **48**, 721 (2008).
[9] T. Hayat, M. U. Qureshi, and N. Ali, Phys. Lett. A **372**, 2653 (2008).
[10] E. F. Elshehawey, N. T. Eldabe, E. M. Elghazy, and A. Ebaid, Appl. Math. Comput. **182**, 140 (2006).
[11] Abd E. Hakeem, Abd E. Naby, A. E. M. El Misery, and F. M. Abd E. Kareem, Physica A **367**, 79 (2006).
[12] M. Kothandapani and Srinivas, Phys. Lett. A **372**, 1265 (2008).
[13] M. Kothandapani and Srinivas, Phys. Lett. A **372**, 4586 (2008).
[14] T. Hayat and N. Ali, Appl. Math. Comput. **193**, 535 (2007).
[15] T. Hayat, M. Javed, and S. Asghar, Phys. Lett. A **372**, 5026 (2008).
[16] S. Srinivas and M. Kothandapani, Int. Comm. Heat Mass Transf. **35**, 514 (2008).
[17] S. Nadeem and N. S. Akbar, Comm. Nonlinear Sci. Numer. Simul. **14**, 3844 (2009).
[18] T. Hayat, N. Ahmad, and N. Ali, Comm. Nonlinear Sci. Numer. Simul. **13**, 1581 (2008).
[19] T. Hayat, N. Alvi, and N. Ali, Nonlinear Anal.: Real World Appl. **9**, 1474 (2008).
[20] M. Kothandapani and S. Srinivas, Int. J. Nonlinear Mech. **43**, 915 (2008).
[21] N. S. Akbar and S. Nadeem, Int. Comm. Heat Mass Transf. **38**, 154 (2011).
[22] N. S. Gad, Appl. Math. Comput. **217**, 4313 (2011).
[23] T. Hayat, M. Javed, and Awatif A. Hedi, Int. J. Heat Mass Transf. **54**, 1615 (2011).
[24] S. Nadeem and N. S. Akbar, Appl. Math. Comput. **216**, 3606 (2010).
[25] A. Ebaid, Phys. Lett. A **372**, 4493 (2008).
[26] D. Tripathi, Acta Astronautica **68**, 1379 (2011).
[27] N. Ali, M. Sajid, Z. Abbas, and T. Javed, European J. Mech.-B/Fluids **29**, 387 (2010).
[28] T. Hayat, M. U. Qureshi, and Q. Hussain, Appl. Math. Modelling **33**, 1862 (2009).
[29] N. S. Akbar, T. Hayat, S. Nadeem, and Awatif A. Hendi, Int. J. Heat Mass Transf. **54**, 1654 (2011).
[30] T. Hayat and S. Hina, Nonlinear Anal.: Real World Appl. **11**, 3155 (2010).
[31] N. Ali, T. Hayat, and M. Sajid, Biorheology **44**, 125 (2007).
[32] T. Hayat, F. M. Mahomed, and S. Asghar, Nonlin. Dynam. **40**, 375 (2005).
[33] M. Mishra and A. R. Rao, Z. Angew. Math. Phys. **54**, 532 (2003).
[34] G. Radhakrishnamacharya, Rheol. Acta **21**, 30 (1982).
[35] A. H. Shapiro, M. Y. Jaffrin, and S. L. Weinberg, J. Fluid Mech. **37**, 799 (1969).
[36] D. Srinivasacharya, M. Mishra, and A. R. Rao, Acta Mech. **161**, 165 (2003).
[37] S. Usha and A. R. Rao, Trans. ASM. J. Biomech. Eng. **199**, 483 (1997).
[38] Y. Wang, T. Hayat, and K. Hutter, Theor. Comput. Fluid Dynam. **21**, 369 (2007).
[39] A. M. Siddiqui, T. Hayat, and M. Khan, J. Phys. Soc. Jpn. **53**, 257 (1994).
[40] N. Ali, Y. Wang, T. Hayat, and M. Oberlack, Biorheology **45**, 611 (2008).